Technical Release No. 6

November 2017

GEFÖRDERT VOM
Bundesministerium für Bildung und Forschung
FONA Resource Land
BMBF

Technical Release No. 6

– The Energy Storage Component –

Andrea Reimuth

This technical release was issued in the context of the project INOLA (Innovations for a sustainable land and energy management on a regional scale) which is funded by the German Federal Ministry of Education and Research (BMBF) in the period from 2014 to 2019. The author(s) is/are responsible for content and results of this release.

Author(s):

Andrea Reimuth (LMU Munich, Department of Geography, research and teaching unit "Physical Geography and Remote Sensing")

Contact:
M.Sc. Andrea Reimuth
Department of Geography
Ludwigs-Maximilians-University Munich
Luisenstr. 37
80333 Munich
E-Mail: a.reimuth@iggf.geo.uni-muenchen.de

All **INOLA-Technical Releases** are available on the project home page www.inola-region.de.

Already published INOLA-Technical releases:

INOLA-Technical Release No. 1:	*INOLA Software Documentation. The Solar Energy Component*
INOLA-Technical Release No. 2:	*INOLA Software Documentation. The Wind Power Component*
INOLA-Technical Release No. 3:	*INOLA Software Documentation. The Hydropower, Geothermal and Environmental Energy Component*
INOLA-Technical Release No. 4:	*INOLA Software Documentation. The Bioenergy Component*
INOLA-Technical Release No. 5:	*INOLA Software Documentation. The Energy Consumption Component*
INOLA-Technical Release No. 6:	*INOLA Software Documentation. The Energy Storage Component*
INOLA-Technical Release No. 7:	*INOLA Software Documentation. The Energy Management Component*
INOLA-Technical Release No. 8:	*INOLA Software Documentation. The Investment Cost Component*

Content

List of Figures

List of Tables

List of Equations

List of Abbreviations

BAT	Battery storage component
BUF	Buffer Storage component
CHEM	Hydrogen and methane storage component
EMOB	Electric mobility component
GSP	Gravity power plant component
PSP	Pumped storage plant component
PTH	Power-to-Heat
SEA	Seasonal Thermal Energy Storage component
SOC	State of charge
STES	Seasonal Thermal Energy Storage

1 Introduction

Energy storage systems will play a more and more important role in the future energy system due to the volatility and inflexibility of the electrical and heat energy production to balance the gaps between energy production and generation. This technical release describes the charging and discharging processes of the storage facilities, whereas the calculation of the energy deltas and the management of the energy system is described in detail in Technical Release No. 7.

Eight man-made storage technologies, which are already in operation or have the potential to be built in the INOLA-region within the next 30 years, are implemented in the PROMET-framework. Depending on the type of conservation the storage plant needs energy in the form of electric power or heat, whereas the power-to-gas systems also generate gas as storage output (see Table 1-1).

Table 1-1: Man-made storage technologies implemented within the Energy Management and Storage Component of the PROMET-framework

Storage Technology	Type of energy input	Type of generated energy	Data format
Pumped-Storage Plants	Electricity	Electricity	.PSP
Gravity Power Plants	Electricity	Electricity	.GSP
Rechargeable Battery Devices	Electricity	Electricity	.BAT
Electric mobility	Electricity	-	.EMOB
Buffer Tanks	Heat	Heat	.BUF
Seasonal Thermal Energy Storages	Heat	Heat	.SEA
Power to Heat	Electricity	Heat	.PTH
Hydrogen and Methane Storage Plants	Electricity	Electricity/Heat/Gas	.CHEM

In the PROMET-environment the storage types are modelled as separate sub models, which are operated by the Storage Management component. Each sub model is generally parameterised by the capacity, the state of charge, the losses from the charging and discharging processes but also in the stand-by mode, the maximum and minimum power and the starting time.

2 The Pumped Storage Power Plant Model

The Pumped Storage Plant Model uses the potential energy by pumping water from a lower to a higher reservoir for charging and turbinating the water when discharging the storage.

Two different model modes are implemented: The first mode considers the hydrological processes with respect to the reservoirs and therefore needs a complete calculation of the water flows within the involved catchments. The second mode calculates the electrical power flows ignoring the hydrological conditions.

2.1 General equations

Both model modes have the same limiting factors for the discharging/charging processes, which are characterised by capacities, efficiency and maximum performance of the pumped storage plant. A further threshold is given by the minimum discharge of the turbine/pump (GIESECKE AND MOSONYI 1998). The potential flow rate, which can be achieved from the power available at each time step, needs to be calculated as shown in Equation (1).

$$Q_{pos} = \frac{P_{pos} \cdot 3600^2 \cdot \Delta t}{1000 \cdot \eta_{P/T} \cdot h \cdot \rho_w \cdot g} \quad (1)$$

with:

Q_{pos}	=	*Potential flow rate through the pump/turbine*	*[m]*
P_{pos}	=	*Available power*	*[MW]*
$\eta_{P/T}$	=	*Efficiency of the pump/turbine*	*[-]*
ρ_w	=	*Density of water*	*[kg/m³]*
h	=	*Elevation difference between upper and lower basin*	*[m]*
Δt	=	*Time step*	*[h]*

As capacity, hourly losses and state of charge depend on the hydrological conditions, the pumped-storage plant model is implemented in two different ways as explained in the following.

2.1.1 Mode 1

At each time step the quantity of available energy and free storage is determined from the water volumes, which are currently stored in the upper and lower reservoirs (see Equation (3)) and the minimum

and maximum water levels. With these parameters the maximum possible performance of the power plant is determined, which can be translated according to the available stored or free capacity.

The water transfer is calculated from the energy available or needed at each time step. The relation between performance and water volume as implemented in the pumped storage plant component is given in equation (2) according to GIESECKE AND MOSONYI (1998).

$$P = \frac{\Delta V \cdot \eta_{P/T} \cdot h \cdot \rho_w \cdot g}{\Delta t \cdot 3600} \quad (2)$$

with:

ΔV	=	*Pumped/turbinated water volume*	*[m³/s]*

The new amount of stored energy is estimated by equation (3) based on GIESECKE AND MOSONYI (1998). The free energy storage is finally calculated in the relation to the capacity of the power plant.

$$E_s = \frac{\left(V_{UR} - \Delta V - V_{\min\_UR}\right)\left(\Delta h + \frac{V_{UR}}{A}\right) \cdot \eta_{P/T} \cdot \rho_w \cdot g}{3.6 \cdot 10^9} \quad (3)$$

with:

E_S	=	*Stored energy*	*[MWh]*
V_{UR}	=	*Water volume of the upper reservoir*	*[m³]*
V_{min_UR}	=	*Minimum water volume*	*[m³]*
A	=	*Area of the upper reservoir*	*[m³]*

2.1.2 Mode 2

In case the hydrological processes are not modelled, the pumped storage plants are initialized with a energy content of 50% of the capacity. The performance, which can be provided by each plant at the time step, is calculated from the quantity of stored and free energy. In addition it is checked if the minimum discharge of the pump/turbine is exceeded (see Equation (1). Meteorological influences like precipitation or the evapotranspiration from the water surface are neglected.

2.2 Pre-processing

2.2.1 Mode 1

The pre-processing includes the identification of the two pixels, at which the outlets of upper and lower reservoirs are situated. Therefore, the reservoirs have to be defined in the dam model and the water transfers in the water transfer model according to WILLEMS, et al. (2007). The pixel of the plant has to

correspond to this of the upper basin. Further data are taken from literature like GIESECKE AND MOSONYI (1998) or STROBL AND ZUNIC (2006).

2.2.2 Mode 2

The data is taken from literature values like GIESECKE AND MOSONYI (1998) and STROBL AND ZUNIC (2006). The pixel of the plant can be determined by overlaying the GIS-Layer with the mask of the model region. The pixel does not necessarily have to represent the geographical location in the grid. However, no further electrical storage plants for can be placed on the selected pixel.

2.3 Input Data and Format

The setup file contains the following sections:

- [General]:

Table 2-1: Description of the input-file for the Pumped Storage Power Plant Model, Section General

Input Parameters	Description	Unit	Data format
PSPName	**Name of the Pumped Storage Power Plant**	**[-]**	**character**
PSPModel	**Model 1 - PSPModel**	**[-]**	**integer**
PSPID	**ID-Number of the Pumped Storage Plant**	**[-]**	**integer**
PSPProxel	**Pixel of the upper reservoir**	**[-]**	**integer**
PSPProxel_UW	**Pixel of the lower reservoir**	**[-]**	**integer**

- [PSP_Model]:

Table 2-2: Description of the input-file for the Pumped Storage Power Plant Model, Section PSP_Model

Input Parameters	Description	Unit	Data format
PSPActive	Status of the Power Plant	[-]	integer
PSPStartyear, PSPStartMonth, PSPStartDay	Start time of the Power Plant	[-]	integer
PSPCapacity	Capacity of the Power Plant	[MWh]	real
Height	Elevation difference between inflow and outflow	[m]	real
nu_t	Efficiency of the turbine	[-]	real
nu_p	Efficiency of the pump	[-]	real
Q_min_t	Minimal discharge of the turbine	[m^3/s]	real
Q_min_p	Minimal discharge of the pump	[m^3/s]	real
P_max_t	Maximum performance of the turbine	[MW]	real
P_max_p	Maximum performance of the pump	[MW]	real

Example setup for the Pumped Storage Power Plant Walchensee:

```
[General]
ObjectType              PSP
PSPName                 Walchenseekraftwerk
PSPModel                1
PSPID                   1
PSPProxel               282     245
PSPProxel_UW            0       0
[end]

[PSP_Model]
PSPActive               1
PSPStartYear            1924
PSPStartMonth           01
PSPStartday             01
PSPCapacity             229750
Height                  200
nu_t                    0.895
nu_p                    999999
Q_min_t                 0.1
Q_min_p                 999999
P_max_t                 72
P_max_p                 0
[end]
```

Figure 2-1: Example of the input file for the Pumped Storage Power Plant Model

If mode 1 is applied, further input data is necessary for the specification of the reservoirs and the water transfer between the basins. For detailed information see WILLEMS, et al. (2007).

2.4 Output

The output of the pumped storage power plant model includes the stored and free capacity in MWh on hourly resolution and the electrical power used for the charging and discharging processes.

3 The Gravity Power Plant Model

The Gravity Power Plants uses a similar storage technology as Pumped Storage Plants though within a closed system: In times of electricity surplus a stone cylinder is hydraulically lifted instead of pumping water upwards in a higher elevated reservoir. With energy deficit, the cylinder presses the stored water back through turbines by sinking down. With this technology a much larger amount of energy can be saved at smaller area than a pumped storage plant independently from the natural landscape conditions (AGRAWAL, et al. 2011, GRAVITY POWER 2017).

3.1 General equations

The Gravity Power Plant model uses a similar approach as the Pumped Storage Plant model:

The charging and discharging power of the gravity storage is again restricted by the maximum performance and the free capacity or the amount of stored energy. As the minimum discharge through the pump/turbine is a further significant limit, the potential flow rate based on the available power is calculated and checked if this threshold is exceeded.

The potential elevation of the weight is determined by the available energy at each time step as shown in Equation (4).

$$\Delta h = \frac{P_{pos} \cdot 3.6 \cdot 10^9}{\eta_{P/T} \cdot \rho_w \cdot g \cdot h_w \cdot r^2 \cdot \pi} \tag{4}$$

with:

Δh	=	*Elevation difference of the weight*	*[m]*
P_{pos}	=	*Available power*	*[MW]*
$\eta_{P/T}$	=	*Efficiency of the pump/turbine*	*[-]*
ρ_w	=	*Density of the weight*	*[kg/m³]*
h_w	=	*Height of the weight*	*[m]*
r	=	*Radius of the weight*	*[m]*

Then the flow rate is calculated from the potential elevation according to Equation (5). In case the minimum flow rates are not exceeded, the gravity power plant cannot store respectively deliver the demanded amount of energy.

$$Q_{P/T} = \Delta h \cdot r^2 \cdot \pi \tag{5}$$

with:

$Q_{P/T}$	=	*Flow rate through the pump/turbine*	*[m³/s]*

The gravity storage is initialized with a charging level of 50% of the capacity. It is further assumed that the gravity power plant has a daily loss rate of 0.05%.

3.2 Pre-processing

The data is taken from literature (GRAVITY POWER 2017, HEINDL ENERGY GMBH 2017) and estimated from pumped storage plants. The pixel of the plant can be determined by overlaying the GIS-Layer with the mask of the model region. The pixel does not necessarily have to represent the geographical location in the grid. However, no further electrical storage plants can be placed on the same pixel.

3.3 Input Data and Format

The setup file contains the following sections:

- [General]:

Table 3-1: Description of the input-file for the Gravity Power Plant Model, Section General

Input Parameters	Description	Unit	Data format
GSPName	**Name of the Gravity Power Plant**	**[-]**	**character**
GSPModel	**Model**	**[-]**	**integer**
GSPID	**ID-Number of the Plant**	**[-]**	**integer**
GSPProxel	**Pixel of the Storage Site**	**[-]**	**integer**

- [GSP_Model]:

Table 3-2: Description of the input-file for the Gravity Power Plant Model, Section GSP_Model

Input Parameters	Description	Unit	Data format
GSPActive	Status of the Power Plant	[-]	integer
GSPStartyear, GSPStartMonth, GSPStartDay	Start time of the Power Plant	[-]	integer
GSPCapacity	Capacity of the Power Plant	[MWh]	real
Radius	Radius of the cylinder	[m]	real
H_cyl	Height of the cylinder	[m]	real
H_tot	Total height of the Power Plant	[m]	real
dens_cyl	Density of the cylinder	[kg/m³]	real
nu_t	Efficiency of the turbine	[-]	real
nu_p	Efficiency of the pump	[-]	real
Q_min_t	Minimal discharge of the turbine	[m³/s]	real
Q_min_p	Minimal discharge of the pump	[m³/s]	real
P_max_t	Maximum performance of the turbine	[MW]	real
P_max_p	Maximum performance of the pump	[MW]	real

Example setup for the Gravity Power Plant in Weilheim:

```
[General]
ObjectType              GSP
GSPName                 Weilheim
GSPModel                1
GSPID                   1
GSPProxel               232     255
[end]

[GSP_Model]
GSPActive               1
GSPStartYear            2018
GSPStartMonth           01
GSPStartDay             01
GSPCapacity             500
Radius                  5
H_cyl                   50
H_tot                   100
Dens_cyl                2600
```

```
nu_t                    0.895
nu_p                    0.786
Q_min_t                 3
Q_min_p                 0
P_max_t                 2
P_max_p                 2
[end]
```

Figure 3-1: Example of the input file for the Gravity Power Plant Model

3.4 Output

The output of the gravity storage model includes the stored and free energy capacity on hourly resolution and the energy used for the charging and discharging processes.

4 The Battery Model

The technology of battery storage systems has been commercially used for a long period in different application modes. The charging and discharging effect of batteries is caused by the flow of electrons due to chemical reactions at the electrodes producing or consuming electrical energy. The battery storage devices available on the German market are characterized by a high variety of capacity, charging behaviour and lifetime, which are dependent on the material combinations and construction form (see C.A.R.M.E.N. E.V. (2017)).

However, within the storage model the term of battery storage system stands for a rechargeable, stationary accumulator, which is always connected to the grid. The applied model approach offers the possibility to simulate several battery types and the associated effects of e.g. differences in performance or the maximum number of cycles.

Three different application modes are implemented in the energy component of the PROMET-software:

- The function of a daily storage device balancing the grid on hourly base, which is managed by the grid operators
- The decentralized option for PV-owners, who want to increase the energy yield of their PV-plants by storing excess energy at home
- The large-scale application for balancing the differences between domestic PV-plants and the energy consumption of villages or small quarters, which have connected to a local energy community

4.1 General equations

The initialization of the battery storage devices includes the following process steps: The maximum power of the rechargeable battery is calculated from the specific energy and specific power of the selected accumulator type. The useable capacity of battery systems directly coupled with PV is set to the corresponding peak power of the photovoltaic sites in kWh as recommended by WENIGER, et al. (2014) obtaining a self-sufficiency level of approximately 60%. The initial energy content of the battery devices is set to 50% state of charge (SOC) of the theoretical capacities.

The simulation of the battery system is based on the simplified approach of WENIGER, et al. (2014). In this model, the dependency of the current on the charging and discharging processes is taken into account simply by a constant efficiency parameter. Further influences like performance and temperature are neglected. The input parameters for different battery types are described in detail in section

4.3.1. The useable battery capacity is restricted to a defined share of the theoretical capacity at the beginning of the lifetime.

The selected approach is extended by the following aspects concerning the capacity and loss rate:

The useable capacity is calculated at each time step as shown in Equation (6).

$$C_t = C_{th} \cdot (1 - (1 - SOC_{tmax}) \cdot nc_{act}/nc_{max}) \quad (6)$$

with:

C_t	=	*Useable capacity at time t*	*[kWh]*
SOC_{tmax}	=	*State of charge at the end of the lifetime*	*[-]*
nc_{act}	=	*Current number of cycles*	*[-]*
nc_{max}	=	*Maximum number of cycles*	*[-]*
C_{th}	=	*Theoretical capacity*	*[kWh]*

The efficiency losses arising due to charging or discharging the battery are considered by an efficiency parameter independently from the power of the batteries. The losses due to the battery management are calculated by an hourly mean related to the theoretical capacity (see Equation (7)).

$$CS_t = CS_t - L \cdot C_{th} \quad (7)$$

with:

CS_t	=	*Stored Energy*	*[MWh]*
L	=	*Loss*	*[-]*
Cth	=	*Theoretical Capacity*	*[km]*

The charging and discharging process is implemented as following:

When charging the battery device, the amount of stored energy is increased by the computed delta regarding the free capacity, the maximum charging power and the efficiency of the process. If the battery is discharged, the amount of stored energy is decreased taking again taking into account the maximum discharging power, the amount of stored energy and the efficiency of the discharging process.

One battery cycle is completed as soon as the battery is recharged after discharging. When the maximum number of cycles is reached the battery is rebuilt with the same parameters but a time delay of three months. The renewed battery devices are specified in the BatDevices.txt-file in the output-folder of the simulation (see Figure 4-1).

For battery systems, which have been built before the start of the model simulation it is assumed, that one battery cycle per day was undergone by the device.

```
##############################################
  Replace BATID          1
  BATName                E2137801000010013002500OS00000001
  BATProxel              27601
  BATType                3
  LoadingStrategy        1
  PV_Coup                1
  nu_Inverter            0.94
  BATCapacity            2.40
  BATStart               01.08.2013
```

Figure 4-1: Specifications of the rebuilt battery devices in the BatDevices.txt-file

4.2 Pre-processing

The data for the battery types is taken from OPIYO (2016) and SCHOOP (2013).

It is possible to place the uncoupled batteries in the grid independently from the geographical location. The battery devices coupled with PV-systems must have the same pixel as the corresponding PV-systems. The pixel for these systems can be determined by overlaying the coordinates of the PV-plant with the pixel layer. The ID-number of the corresponding PV-system must be similar with the position within the PV-list. The capacity of the coupled battery system is automatically calculated by the model and therefore cannot be entered manually.

4.3 Input Data and Format

The battery model is described by two input files: The first file defines the physical characteristics of the different accumulator types in general. The second file includes information about the batteries, which are used for the storage processes.

The input for battery devices, which are located centralized in the grid, supplying villages or small quarters, includes the amount of affected households and non-residential energy consumers as well as the PV-systems, which are part of this energy community. A detailed description of the additional input file needed for this storage application is given in Technical Release No. 7.

4.3.1 Battery Types

This setup file only needs one keyword for the description of each type:

- [BatteryType]:

Table 4-1: Description of the input-file for the Battery Type Model, Section BatteryType

Input Parameters	Description	Unit	Data format
Name	Name of the battery type	[-]	character
Model	Model number	[-]	integer
NomVoltage	Nominal Voltage of the Battery Type	[V]	real
Spec.Energy	Specific Nominal Energy related to the mass of the battery	[Wh/kg]	real
Spec.Power	Specific Nominal Power related to the mass of the battery	[W/kg]	real
Efficiency	Efficiency of the charging/discharging process	[-]	real
NoCycles	Maximum number of cycles	[-]	integer
LevelmaxCycle	State of charge at the end of the lifetime	[-]	real
UseCap	Useable Capacity related to theoretical capacity	[-]	real
Lifetime	Lifetime of the Battery type	[a]	integer
Losses	Hourly Losses related to the theoretical capacity	[-]	real

Example setup for the Lithium-Ion Battery:

```
[BatteryType]
ObjectType              BAT
Name                    LiIon-HighEnergy
Model                   1
NomVoltage              3.6
Spec.Energy             170
Spec.Power              50
Efficiency              0.99
NoCycles                3000
LevelMaxCycle           0.90
UseCap                  0.40
Lifetime                20
Losses                  0.00000625
[end]
```

Figure 4-2: Example of the input file for the Battery Type Model

4.3.2 Battery Devices

The setup file for the battery devices is split into the following sections:

- [General]:

Table 4-2: Description of the input-file for the Battery Model, Section General

Input Parameters	Description	Unit	Data format
ObjectName	Name of the battery device	[-]	character
BATID	ID-number of the battery device	[-]	integer
BATProxel	Pixel	[-]	integer

- [Bat_Model]:

Table 4-3: Description of the input-file for the Battery Model, Section Bat_Model

Input Parameters	Description	Unit	Data format
BATActive	Status of the Battery Device 0 – off, 1 – on	[-]	integer
BATType	ID-Number of the BatteryType	[-]	integer
LoadingStrat	Loading Strategy of the Battery Device	[-]	integer
nu_Inverter	Efficiency of the power inverter	[-]	real
PV_coup	Status of Coupling: 0 – centralized and managed by grid operators, 1 – decentralized and coupled to PV-system, 2 – centralized and coupled to neighbourhood energy community	[-]	integer
PV_ID	ID-number of the coupled PV-system	[-]	integer
BatteryStartYear, BatteryStartMonth, BatteryStartDay	Start time of the Battery device	[-]	integer
Capacity	Capacity of non-coupled battery devices	[kW]	real

Example setup for the Lithium-Ion Battery:

```
[General]
BATType                 bat
BATName                 E213780100001001300250005000000001
BATID                   1
BATProxel               113    733
[end]
```

```
[Battery_Model]
BATActive               1
BATType                 1
LoadingStrat            1
nu_Inverter             0.94
PV_coup                 1
PV_ID                   2
BATStartYear            1996
BATStartMonth           11
BATStartDay             13
BATCapacity             0
[end]
```

Figure 4-3: Example of the input file for the Battery Model

4.4 Output

The results of the battery model include location, state of charge, free storage, performance, the grid exchange, the feed-in limits of the grid per hour on pixel scale as well as the amount of battery devices per pixel.

5 The Electric Mobility Model

The increasing number of electric cars offers a further storage possibility in times of excessive power. In this component the batteries of electric cars can only be used for charging as a possibility to reduce the amount of excessive electric energy. The reason for this is that each discharging process would lead to ageing of the battery, which could result in a significantly shorter lifespan in case of the management by grid owners. Because of higher demands, battery systems for cars are more expensive than those used for photovoltaic systems, so that a shorter life time would lead to higher costs. For this reason, the support of grids in times of energy deficit is currently not profitable (JÜLICH, et al. 2016).

5.1 General equations

The availability of the chargeable capacity of electric cars is influenced by two aspects: The stock of electric vehicles with different battery sizes and the number of cars, which are connected to the grid at the current time step.

The stock of electric cars is determined by the number of cars per capita for three different categories of electrical driven vehicles, which are read in for selected years (see chapter 5.3 for further details of the input). The current stock B_i is then calculated on yearly resolution by linear interpolation of the values, which are finally referred to the according population number.

The available total capacity C_{av} is calculated according to Equation (8), which neglects the influence of commuters.

$$C_{av} = \left(B_1 \cdot C_{m\_1} + B_2 \cdot C_{m\_2} + B_3 \cdot C_{m\_3}\right) \cdot \frac{P_{act}}{3600} \tag{8}$$

with:

C_{av}	=	*Available Capacity*	*[MWh]*
B_i	=	*Vehicle Stock of type i*	*[-]*
C_{m_i}	=	*Average Battery Capacity of vehicle type i*	*[km]*
P_{act}	=	*Current population number*	*[-]*

The number of cars, which are connected to the grid and accessible for charging the batteries, is defined as shown in equation (9).

$$C_{acc\_t} = C_{av} \cdot \left(S_1 \cdot SOC_1 \cdot CT_{1\_t} + S_2 \cdot SOC_2 \cdot CT_{2\_t}\right) \tag{9}$$

with:

C_{acc}	=	*Capacity accessible to the grid*	*[MWh]*
S_i	=	*Share of private/business vehicles*	*[-]*
SOC_i	=	*Average state of charge of private/business vehicles*	*[-]*
CT_{i_t}	=	*Percentage of vehicles connected to the grid at hour t*	*[-]*

The average battery capacity is dependent on the maximum distance, which can be covered electrically, and on the energy consumption, which is also linearly interpolated from data for different input years.

$$C_{m\_i} = D_i \cdot CS_i \tag{10}$$

with:

C_{m_i}	=	*Average Capacity*	*[MWh]*
D_i	=	*Battery Distance of vehicle type i*	*[km]*
CS_i	=	*Electric energy demand of vehicle type i*	*[MJ/km]*

The total charging power, which can be taken from the available electric cars, is finally determined according to Equation (11):

$$P = E_{pos} \cdot \eta_{ch} \tag{11}$$

with:

P	=	*Total charging Power*	*[MW]*
E_{pos}	=	*Energy surplus from the grid limited by the accessible capacity* C_{acc_t}	*[MWh]*
η_{ch}	=	*Efficiency of the charging power*	*[-]*
P	=	*Total charging Power*	*[MW]*

5.2 Pre-processing

The data for the share of private/commercial vehicles, the charging times and the average state of charge of the batteries are taken from FRENZEL, et al. (2015). The energy demand, efficiencies and the vehicle stock are taken from HACKER, et al. (2014)

The pixel only serves as output path for the whole simulated area and can be chosen independently from the geographical location.

5.3 Input Data and Format

The electric mobility file contains the following four keywords:

- [Vehicle_Model]:

Table 5-1: Description of the input-file for the Electric Mobility Model, Section Vehicle_Model

Input Parameters	Description	Unit	Data format
Proxel	Pixel	[-]	integer
EmobActive	Status of the Electric Mobility Component	[-]	integer
Distance	Distance of the three different vehicle types	[km]	integer
Years_EnCons	Amount of reference years for the development of the electric consumption	[-]	integer
Years, ECnons	Year and Energy consumption per vehicle type	[MJ/km]	real

- [Vehicle_Stock]:

Table 5-2: Description of the input-file for the Electric Mobility Model, Section Vehicle_Stock

Input Parameters	Description	Unit	Data format
Years_VehStock	Amount of reference years for the development of the vehicle stock	[-]	integer
Year, VehStock	Year and Vehicle Stock per vehicle type per Capita	[pC]	real

- [Charging_Model]:

Table 5-3: Description of the input-file for the Electric Mobility Model, Section Charging_Model

Input Parameters	Description	Unit	Data format
Share	Share of private and business electric vehicles	[-]	real
State of charge	Average state of charge for the two types of use	[-]	real
nu	Efficiency of the charging process	[-]	real

- [Charging_Time]:

Table 5-4: Description of the input-file for the Electric Mobility Model, Section Charging_Time

Input Parameters	Description	Unit	Data format
Hours	**Amount of reference hours for the share of vehicles connected to the net per type of use**	**[-]**	**real**
Hour, VehCon	**Hour and share of vehicles connected to the grid**	**[-]**	**real**

Example setup for the electric mobility component:

```
[Vehicle_Model]
Proxel                  41    308
EMobActive              1
Distance                225       100            50
Years_EnCons            5
2010                    0.71      0.67           0.67
2020                    0.59      0.56           0.56
2030                    0.53      0.53           0.54
2040                    0.46      0.46           0.47
2050                    0.42      0.42           0.43
[end]

[Vehicle_Stock]
Years_VehStock          4
2020                    0.005357883   0.007061688   0.006230093
2030                    0.029954647   0.023467839   0.030497792
2040                    0.201958792   0.042014461   0.078126060
2050                    0.391278271   0.041051992   0.098251929
[end]

[Charging_Model]
Share                   0.63     0.37
State of Charge         0.32     0.25
Nu                      0.9
[end]

[Charging_Time]
Hours                   8
0                       0.0475   0.0425
2                       0.0233   0.0267
5                       0.0300   0.0300
7                       0.0400   0.0580
12                      0.0533   0.0567
15                      0.0800   0.1033
18                      0.1275   0.1150
22                      0.0475   0.0425
[end]
```

Figure 5-1: Example for the input file of the Electric Mobility Model

Output

The output of the electric mobility component includes the free capacity of these cars, which are connected to the grid, the energy used for charging and the general battery capacity of the current automobile stock.

6 The Buffer Storage Model

This type stores the energy in the form of sensible heat using water as storage medium. Thus, buffer tanks can be coupled to any source of heat energy like waste heat or power-to-heat systems.

For this storage type two different application scales are common: Very often the energy delta of the heating system and the consumption of autonomously supplied buildings is balanced by buffer tanks. The reason for this is a higher solar yield or the decrease of the starting processes of boilers or heat pumps.

Apart from this buffer storages are commonly used in local heat networks: Since the central heating systems like cogeneration plants normally cannot immediately response to short-time changes of the consumers, buffer storages serve as additional balancing component apart from the grid. In this function they can also serve as the link to further storage types like seasonal heat storages.

6.1 General Equations

A well performing buffer storage normally shows a strong layering of the water with different temperatures (FLOß AND DIETRICH). However, the model used to simulate the storage processes is based on the assumption of an ideally mixed tank due to simplicity reasons. Thus, the water density, the heat capacity and the temperature profile are modelled as constants in vertical and horizontal direction. The averaging of the buffer temperature leads to a temporal shift of the discharging process as the excess temperatures of the heating system is reached at a later time step. However, it is then exceeded for a longer time span (PETER 2013).

6.1.1 Initialization of the buffer tanks for domestic applications

The water volume for buffer tanks used for the heating support on domestic level are calculated according to Equation (12). The coefficients for the two heating systems are listed in Table 6-1. It is assumed that the minimum water volume for the buffer tanks cannot fall below 400 l as recommended by DIN 4708-2 for apartment houses.

$$V_{buf} = A_{ST}(P_{HS}) \cdot f_{HS} \tag{12}$$

with:

V_{buf}	=	*Water volume of the buffer tank*	*[l]*
A_{ST}/P_{HS}	=	*Area of the solar thermal system/ Maximum Performance of the heating system*	*[m²] / [kW]*
f_{HS}	=	*Coefficient for the heating system of the buffer tank*	*[l/m²] / [l/kw]*

Table 6-1: Coefficients of the different heating systems used to calculate the water volume of the buffer tank

Heating system	f_{HS} [l/m²] / [l/kW]	Source of f_{HS}
Solar thermal energy combined with pellet heating	**65**	**SCHABBACH AND LEIBBRANDT (2014)**
Heat pump	**25**	**OCHSNER (2009)**

The maximum capacity of the buffer storage is determined by the selected water volume as shown in Equation (13). It is assumed that the buffer storage can reach a maximum temperature of 95 °C.

$$C_{buf} = V_{buf} \cdot cw \cdot \frac{t_{max}}{3.6 \cdot 10^6} \quad (13)$$

with:

C_{buf}	=	*Storage capacity of the buffer tank*	*[kWh]*
cw	=	*Specific heat capacity of water*	*[J/kg °C]*
t_{max}	=	*Maximum temperature of 95°C*	*[°C]*

The minimum energy that has to be kept by the buffer storage to secure a gapless supply is dependent on the heating system. For underfloor or wall heating systems a minimum temperature of 35 °C is enough, whereas radiators and systems with drinking water heating are assumed to need a minimum temperature of 60 °C in the upper third of the buffer tank (SCHABBACH AND LEIBBRANDT 2014). It is furthermore assumed that the water temperature of the inflow of the buffer tank has a constant temperature of 12 °C. Equation (14) is used for the heating systems needing a low nominal inflow temperature, whereas Equation (15) shows the calculation of the minimum energy for radiators and drinking water heating systems with an equally distributed layering of 60 °C, 40 °C and 20 °C.

$$E_{min} = V_{buf} \cdot (35 - t_{Wi}) \frac{1.16}{10^3} \quad (14)$$

$$E_{min} = \frac{V_{buf}}{3} \cdot (60 + 40 + 20 - 3t_{Wi}) \cdot \frac{1.16}{10^3} \quad (15)$$

with:

E_{min}	=	*Minimum energy content that has to be kept by the buffer tank*	*[kWh]*
t_{Wi}	=	*Temperature of the inflow water*	*[°C]*

The initial energy content of the buffer storages is set to 50% of their capacities.

6.1.2 Initialization of the buffer tanks for local heat networks

The buffer tanks coupled with central heating systems and heat networks, which supply more than one household or business enterprise, are subjected to various conditions depending on the amount of connected buildings and the types of heating systems. Therefore, the water volume is part of the input as described in Chapter 6.3. The maximum capacity is determined according to Equation (13). The initial energy content of the buffer storages is set to 50% of their capacities.

6.1.3 Operation of the buffer tanks

The heat losses of the buffer storage are mainly dependent on the temperature difference between ambient air and water content and the insolation of the buffer tank. They are calculated at each time step before the buffer storage is charged or discharged

The heat loss rate is calculated with an exponential function with the water volume as the only variable (see Equation (16)). The determination of parameters is based on data from PETER (2013) (see Appendix Table A 1).

$$LR = p_F \cdot V_{buf}{}^{0,5927} \tag{16}$$

with:

LR	=	*Heat loss rate*	*[W/K]*
p_F	=	*Form parameter of* 0.0587	*[W/Km³]*

The hourly losses are calculated according to Equation (17) and Equation (18). It is assumed that the buffer storage is positioned in the cellar of the building with a constant temperature of 15 °C according to DIN EN 12831-1 Supplement 2 Table 2.

$$\Delta T_{buf} = \frac{C_{ges}}{V_{buf} \cdot cw} \cdot 3.6 \cdot 10^6 - T_a \tag{17}$$

$$L_{buf} = \left(\Delta T_{buf} + 273.15\right) \cdot LR \tag{18}$$

with:

ΔT_{buf}	=	*Difference of buffer and ambient temperature*	*[°C]*
C_{ges}	=	*Stored energy in the buffer tank*	*[kWh]*
T_a	=	*Ambient temperature (assumed to be 15°C)*	*[°C]*

The limiting factors for charging performance of the buffer tank are the free capacity or stored energy and the minimum temperature difference between tank and the heat energy from the solar thermal

panels. The circulation pump of the solar system starts, when the energy difference of the two carrier fluids exceeds at least 7 °C (see Equation (19)). If the circulation pump had already started in the time step before, a minimum difference of only 3 °C is necessary for the heat transfer from the panels to the buffer tank (SCHABBACH AND LEIBBRANDT 2014). It is assumed that the inlet of the heat source is within the lower part of the buffer tank, so that the threshold is determined only based on one third of the buffer volume.

$$E_{dif} = \Delta T_{Cmin} \cdot \frac{V_{buf}}{3} \cdot \frac{cw}{3.6 \cdot 10^6} \quad (19)$$

with:

E_{dif}	=	*Minimum energy difference needed for the circulation pump*	*[kWh]*
ΔT_{Cmin}	=	*Temperature difference of 3 °C/7 °C*	*[°C]*

In contrast, the discharging process of the buffer tank is only limited by the current heat content. Since the supply with heat has to be gapless for heating systems for single consumers, the minimum energy content of the buffer tank has to be exceeded at each time step. The heat pump is activated when the heat content of the buffer tank falls below this threshold. For a solar heat system, this is ensured by a pellet heating system, which guarantees the heat supply in times of insufficient sunshine.

6.2 Pre-processing

The efficiency of the buffer tanks is assumed to 94 %.

It is possible to place the buffer storages, which are connected to local heat networks in the grid independently from the geographical location. The buffer tanks coupled with a domestic solar thermal plant or heat pump must have the same pixel as the corresponding heat production unit. The pixel for these systems can be determined by overlaying the coordinates of the heat production site with the pixel layer. The ID-number of the corresponding heat production-system must be similar with the position within the corresponding list. The capacity of the buffer tanks coupled to a domestic solar thermal plant, heat pump is calculated automatically and cannot be entered manually.

6.3 Input data and Format

The setup file for buffer tanks is split into the following two sections:

- [General]:

Table 6-2: Description of the input-file for the Buffer Storage-Model, Section General

Input Parameters	Description	Unit	Data format
BUFName	**Name of the Buffer tank**	**[-]**	**character**
BUFModel	**Model of the Buffer tank**	**[-]**	**integer**
BUFID	**ID-number of the Buffer tank**	**[-]**	**integer**
BUFProxel	**Pixel**	**[-]**	**integer**

- [BUF_Model]:

Table 6-3: Description of the input-file for the Buffer tank-model, Section BUF_Model

Input Parameters	Description	Unit	Data format
BUFActive	**Status of the Buffer tank, 0 – off, 1 – on**	**[-]**	**integer**
BUFStartYear, BUFStartMonth, BUFStartDay	**Start time of the Buffer tank**	**[-]**	**integer**
BUFCapacity	**Capacity of the buffer tank**	**[kWh]**	**real**
BUFType	**Type of the buffer tank, 1 – domestic, 2 – industrial application**	**[-]**	**real**
nu	**Efficiency of the charging and discharging process**	**[-]**	**real**
BUF_TW	**0 – underfloor or wall heating system without drinking water heating, 1 – radiator heating system and/or drinking water heating system**	**[-]**	**integer**
BUF_Coup	**Type of heat production unit, 1 – solar thermal, 2 – heat pump, 0 - local heat network**	**[-]**	**integer**
BUF_CoupID	**ID-number of the production unit**	**[-]**	**integer**

Example setup for a Buffer tank coupled to a domestic solar thermal plant:

```
[General]
ObjectType              BUF
BUFName                 E213780100001001300250005000000001
BUFModel                1
BUFID                   1
Position_Proxel         113    733
[end]

[BUF_Model]
BUFActive               1
BUFStartYear            1996
BUFStartMonth           11
BUFStartDay             13
BUFCapacity             0
nu                      0.94
BUF_TW                  1
BUF_Coup                1
BUF_CoupID              2
 [end]
```

Figure 6-1: Example of the input file for the Buffer tank

6.4 Output

The output includes the free storage capacity and amount of saved energy of the buffer tank as well as the performance at each time step. For solar-based heating systems, the energy demand of the wood-fired heating is also calculated.

7 The Seasonal Thermal Energy Storage Model

Seasonal thermal energy storages (STES) are a storage option of thermal energy, which is suitable for local heat networks with a high share of solar thermal energy production. This technology balances the frequent excess production of thermal energy in the summer months and the increased energy demand in the winter season.

Four different types of STES-plants are modelled in this component:

- the Hot Water STES-plant, which works similar to a buffer tank
- the gravel-water STES-plant, that combines water with gravel-stones as storage media
- the borehole STES-plant, which uses the storage capacity of the soil
- The aquifer STES-plant, that stores the excess thermal energy in groundwater systems

7.1 General equations

The initialization of the STES-plant includes the calculation of the storage capacity as shown in Equation (20). The capacity factors, which depend on the storage media of the four implemented types, are taken from MANGOLD, et al. (2001) (see Appendix Table A 2). The STES-plants are initialized with an energy content of 50% of the calculated capacity. The effects of the settling time in the first years after the start of operation on the efficiency are neglected.

$$C_{SHS} = V_{SHS} \cdot p_{ST} \tag{20}$$

with:

C_{SHS}	=	*Capacity of the seasonal heat storage plant*	*[kWh]*
V_{SHS}	=	*Volume of the storage plant*	*[m³]*
p_{ST}	=	*Storage capacity per m³*	*[kWh/m³]*

The losses of the STES-plants are calculated on hourly resolution. As the STES-plants are normally located below the surface because of a better insulation, the temperature of the first soil layer is assumed to be the temperature of the complete surrounding surface.

Similar to the Buffer Storage model described in chapter 6, the STES-model is based on the assumption of an ideally mixed tank. Therefore, the temperature determined according to Equation (21) is the average value for the water volume of the STES-plant. The volumes of the the gravel-water-, the borehole-, or the aquifer STES-plants are converted to the water equivalent according to Appendix Table A 3.

$$T_{STES} = \frac{E_{Hs} \cdot 3600}{V_{STS} \cdot sv \cdot cw} + 273.15 \quad (21)$$

with:

T_{STES}	=	*Temperature of the STES-plant*	*[K]*
E_{Hs}	=	*Amount of saved energy*	*[kWh]*
V_{STS}	=	*Volume of the storage plant*	*[m³]*
sv	=	*Storage volume for 1 m³ water equivalent*	*[-]*

The losses are determined according to Equation (22) using the average thermal energy conductivity of the surface insulation of the STES-plant.

$$L_{SHS} = \frac{(T_{Sl} - T_{STES}) \cdot \lambda_{STES}}{1000} \quad (22)$$

with:

L_{SHS}	=	*Loss*	*[kWh]*
T_{Sl}	=	*Temperature of the first soil layer*	*[K]*
λ_{STES}	=	*Average thermal conductivity of the insulation*	*[W/K]*

The charging performance of the STES-plant is limited by the available excess thermal energy in the local heat network system, the efficiency of the charging process and the free capacity.

Limiting factors for the discharging process are the discharge efficiency and the amount of stored energy. If the energy content of STES-plant drops below 40% of the capacity, it is assumed that the water temperature in the storage can no longer exceed a value of 65 °C, which is the inlet temperature of the local heat network. This threshold value is based on the existing STES-plant in Munich, Ackermannbogen (see HAUER, et al. (2013)).

If no additional heating is installed within the STES-plant, the supply with thermal energy ceases at this point.

If an additional heating system is integrated into the STES-plant, the energy needed to reach the temperature level of 65 °C is supplied by electrical heating systems like heat pumps or power-to-heat.

Because of neglecting the layered temperature profiles, it is not possible to determine the energy consumption of the additional heating system in detail. So, for simplicity reasons, a constant efficiency is assumed depending on the amount of energy that is discharged (see Equation (23)).

$$P_{HP\_STES} = P_{STES}/\eta_{AHS} \quad (23)$$

with:

P_{HP_STES}	=	*Energy demand for the additional heating system*	*[kWh]*
P_{STES}	=	*Amount of discharged thermal energy at hour t*	*[kWh]*
η_{AHS}	=	*Efficiency of the additional heating system*	*[-]*

7.2 Pre-processing

The data is taken from literature (MANGOLD, et al. 2001, HAUER, et al. 2013, SOLITES 2014).

The pixel of the STES-plant can be determined by overlaying the GIS-Layer with the mask of the model region. The pixel does not necessarily have to represent the geographical location in the grid. However, no further thermal energy storage systems can be placed on the same pixel. The STES-plant has to be coupled to a local heat network and combined with a buffer storage and at least one heating system.

7.3 Input data and Format

The setup file for the STES-plant is split into the following sections:

- [General]:

Table 7-1: Description of the input-file for the Seasonal Thermal Energy Storage-Model, Section General

Input Parameters	Description	Unit	Data format
SEAName	**Name of the STES-plant**	**[-]**	**character**
SEAModel	**Model of the seasonal STES-plant: 0 – no add. Heating systems, 1 – with add. heating system**	**[-]**	**integer**
SEAID	**ID-number of the seasonal STES-plant**	**[-]**	**integer**
SEAProxel	**Pixel**	**[-]**	**integer**

- [SEA_Model]:

Table 7-2: Description of the input-file for the Seasonal Thermal Energy Storage-model, Section SEA_Model

Input Parameters	Description	Unit	Data format
SEAActive	Status of STES-plant: 0 – off, 1 – on	[-]	integer
SEAStartYear, SEAStartMonth, SEAStartDay	Start time of the STES-plant	[-]	integer
SEAType	Type of the STES-plant: 1 – Hot water STES, 2 – gravel-water STES, 3 – Borehole STES, 4 – Aquifer STES	[-]	integer
SEAVolume	Volume of the STES-plant	[m^3]	real
SEAInsulation	Average thermal conductivity of the insulation	[W/K]	real
nu_Charge	Thermal Efficiency of the heat charger at charging	[-]	real
nu_Discharge	Thermal efficiency of the heat charger at discharging	[-]	real
nu_HP	Electrical efficiency of the additional heating system to reach the nominal temperature	[-]	real

Example setup for a STES-plant:

```
[General]
ObjectType              SEA
SEAName                 Ackermannbogen
SEAModel                1
SEAID                   1
SEAProxel               282     245
[end]

[SEA_Model]
SEAActive               1
SEAStartyear            2000
SEAStartMonth           1
SEAStartDay             1
SEAType                 1
SEAVolume               10000
SEAInsulation           0.245
nu_charge               0.8
nu_discharge            0.95
nu_HP                   0.8
[end]
```

Figure 7-1: Example of the input file for the Seasonal Thermal Energy Storage Plant

7.4 Output

The output includes the free storage capacity and amount of saved energy of the STES-plant as well as the transferred heat performance and potentially the energy consumption of the additional heating system at each time step.

8 The Power-to-Heat Model

A Power-to-Heat (PTH) system enables the transformation of electrical power to thermal energy. Here, the PTH-model has the function of reducing the energy surpluses in the electric grid. The operation of PTH-plants with the goal of securing the supply of the thermal energy demand is not considered by this storage type. For this reason, the PTH-systems have to be coupled with buffer tanks and with a regulating heat production unit to balance demand and supply. The coupling with local heat networks and STES-plants sites can lead to stronger grid balancing effects of the power-to-heat systems.

8.1 General equations

As the PTH-system is only activated in hours of a surplus of electric energy, the PTH-component can only charge the buffer tank from the negative energy deltas in the grid. The electrical energy transformed to heat is limited by the maximum performance of the PTH-system and the free capacity of the corresponding buffer tank. The losses from to the energy conversion are calculated according to Equation (24).

$$E_W = P_{av} \cdot \eta_{PTH} \tag{24}$$

with:

E_W	=	*Amount of produced thermal energy*	*[kW]*
P_{av}	=	*Available Power at hour t*	*[kW]*
η_{PTH}	=	*Efficiency of the PTH-system*	*[-]*

8.2 Pre-processing

The data is taken from literature (STERNER AND STADLER 2014). The pixel of the plant can be determined by overlaying the GIS-Layer with the mask of the model region. The pixel does not necessarily have to represent the geographical location in the grid. However, no further electrical and STES-plants can be placed on the same pixel. The ID-number of the corresponding buffer tank must be similar with its position within the Buffer storage list (details of the input for the buffer tanks are specified in chapter 6.3).

8.3 Input Data and Format

The setup file for the Power-to-heat systems is split into the following sections:

- [General]:

Table 8-1: Description of the input-file for the PTH-Model, Section General

Input Parameters	Description	Unit	Data format
ObjectName	Name of the PTH system	[-]	character
PTHID	ID-number of the PTH system	[-]	integer
PTHProxel	Pixel	[-]	integer

- [PTH_Model]:

Table 8-2: Description of the input-file for the PTH-model, Section PTH_Model

Input Parameters	Description	Unit	Data format
PTHActive	Status of PTH system 0 – off, 1 – on	[-]	integer
PTHType	Model type of the PTH-system	[-]	integer
StorageID	ID-number of the corresponding Buffer tank	[-]	integer
BatteryStartYear, BatteryStartMonth, BatteryStartDay	Start time of the PTH-system	[-]	integer
P_max	Maximum performance of the PTH-system	[kW]	real
nu	Efficiency of the PTH-system	[-]	integer

Example setup for a PTH-system:

```
[General]
ObjectType              PTH
PTHName                 NahwaermeBadToelz
PTHModel                1
PTHID                   1
PTHProxel               282     245
[end]

[PTH_Model]
PTHActive               1
PTHType                 1
StorageID               5
Startyear               1990
StartMonth              1
StartDay                1
P_max                   5000
nu                      0.95
[end]
```

Figure 8-1: Example of the input file for the Power-to-Heat system

8.4 Output

The output includes the amount of consumed electric energy, the free storage capacity and the amount of saved energy of the corresponding buffer tanks.

9 The Hydrogen and Methane Storage Model

The production of hydrogen and methane from surplus electrical or organically bounded energy offers several paths of storing it as energy carrier and converting it back to electrical power and heat. The energy flows implemented in this component are depicted in Figure 9-1. The storage model used in this component focusses on the technical applications of the gas generation and utilization. The bio-chemical production of the two fuels by bacteria within the biogas plants is not implemented here.

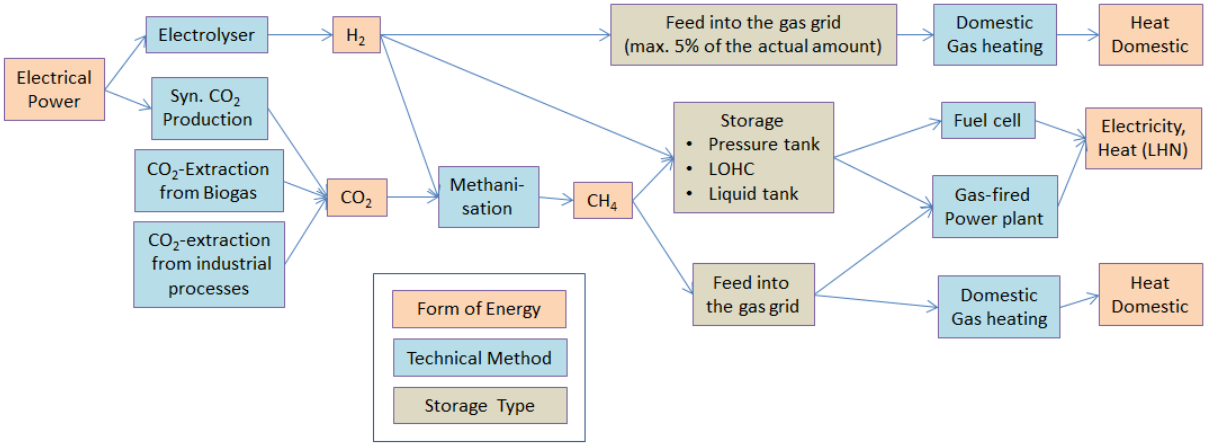

Figure 9-1: Energy paths of the hydrogen and methane storage plant model

9.1 General equations

As the gas pipes and their different pressure limits are not part of the current model environment, the infrastructure for feed-in of the relevant plants into the gas grid is assumed already adequate.

The hourly losses of the storage facilities are calculated at each time step according to Equation (25).

$$L = CH_{St} \cdot lr_F \tag{25}$$

with:

L	=	*Total Loss*	*[kWh]*
CH_{St}	=	*Amount of stored energy*	*[kWh]*
lr_F	=	*Hourly Loss rate of the hydrogen or methane storage*	*[-]*

9.1.1 The Production and Storage of Hydrogen and Methane

The hydrogen production is limited by the minimum and maximum performance of the electrolyser, the losses of the rectifier, the excess energy in the grid and the free storage capacity. For a feed-in of the gas into the gas grid, the hourly demand of the model region is assumed to be the total capacity of the grid; the further storage options offered by the gas network like cavern storage facilities or variations of the gas pressure are not considered by this component.

The amount of hydrogen that can be stored and/or transmitted by the grid (also in the form of methane) is determined according to Equation (26) depending on the facilities of the plant. It is generally assumed that two mole of hydrogen are needed to produce one mole of methane.

$$H_{2pos} = H_{2F1} \cdot (H_{2Ct} + k \cdot C_{GG}) + \frac{stm}{H_{2F2} \cdot CH_{4hV}} \cdot (CH_{4Ct} + (1-k) \cdot C_{GG}) \quad (26)$$

with:

H_{2pos}	=	*Maximum amount of hydrogen that can be produced at time step t*	*[Nm³]*
H_{2F1}	=	*Conversion factor of hydrogen 3.00*	*[kW/Nm³]*
H_{2Ct}	=	*Free capacity of the Hydrogen storage*	*[kWh]*
C_{GG}	=	*Gas demand at hour t*	*[kW]*
H_{2F2}	=	*Density of hydrogen of 0.0899*	*[kg/Nm³]*
CH_{4Ct}	=	*Free capacity of Methane storage*	*[kWh]*
stm	=	*stoichiometric factor of 2*	*[-]*
CH_{4hV}	=	*Caloric Heat value of methane of 15.4*	*[kWh/kg]*
k	=	*Percentage of Feed-in of hydrogen into the gas grid: 0 if no, or 0.05 if yes*	*[-]*

The electrolyser model is based on the assumption of a linear dependency of the performance and the production rate of hydrogen as depicted in Figure 9-2. The production of hydrogen is only limited by the minimum and maximum performance of the electrolyser. Thus, the efficiency of the electrolysis is given indirectly by the production rate. Further influences on the production rate, e.g. the temperature, pressure or the current-voltage relationship, are neglected for reasons of simplicity.

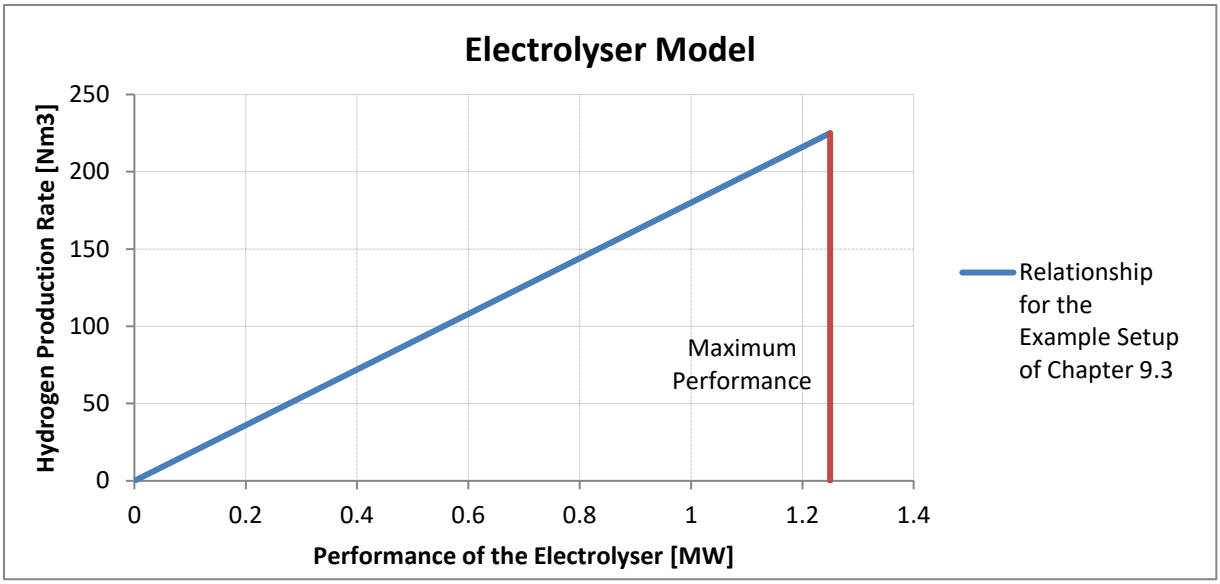

Figure 9-2: Relationship between the hydrogen production rate and the performance of the electrolyser model shown for the Example of Chapter 9.3.

Based on this model, the electrical energy needed to transform the storable hydrogen H_{2pos} is calculated at each time step as shown in Equation (27). The energy losses due to the storing processes and/or the transformation to methane are already considered by the efficiency η_{St}.

$$E_{pos} = \left(\left(H_{2pos} - H_{2min}\right) \cdot \frac{(P_{nom}(1 - P_{min})}{(H_{2nom} - H_{2min})} + P_{nom} \cdot P_{min} \right) / \eta_{St} \qquad (27)$$

with:

E_{pos}	=	*Electric energy that can be transformed according to the free storage and grid capacities*	*[kWh]*
H_{2min}	=	*production rate of the electrolyser at minimum performance*	*[Nm³]*
P_{nom}	=	*Nominal performance of the electrolyser*	*[kW]*
P_{min}	=	*Minimum performance related to the nominal performance of the electrolyser*	*[kW]*
H_{2nom}	=	*Hydrogen production rate at nominal performance*	*[Nm³]*
η_{St}	=	*Efficiency of the hydrogen storage/Sabatier process*	*[-]*

The electrical energy, which can be stored by the hydrogen and methane facility, is further restricted by the available energy surplus and the minimum or maximum performance of the electrolyser.

With these restrictions, the final hydrogen and methane production is assessed from the determined power based on the linear relationship between the hydrogen production rate and the electrolyser performance (see Equation (27)).

If the plant is connected to the gas grid, the gas demand is first covered by the produced hydrogen and methane before the storage facility is filled.

9.1.2 The Consumption of Hydrogen and Methane

The consumption model is applicable for fuel cells and gas-fired plants. Depending on the type of the stored fuel, the power plant has to be adapted to the properties of the hydrogen respectively methane gas. It is assumed that the power plants are ready for operation, so that gaps in the electrical energy production can be closed immediately within one hour. Start-up times and losses due to stand-by modes are neglected.

The generation of electrical power is limited by the minimum and maximum performance, the efficiency of the transformation process and the amount of stored energy.

For power plants like high-temperature fuel cells, the waste heat can serve as an additional source of thermal energy production. The amount of thermal energy, which arises in times of electricity generation, is determined as shown in Equation (28). The additional heat generation after operation of the plant is neglected in this model.

$$E_{wh} = E_C \cdot \eta_{wh} \tag{28}$$

with:

E_{wh}	=	*Amount of produced waste heat*	*[kWh]*
E_C	=	*Amount of produced electrical energy*	*[kWh]*
η_{wh}	=	*Share of waste heat*	*[-]*

9.1.3 Calculation of the lifetime of the system components

As defined in the input file, the three components of a hydrogen and methane power plant have an individually specified lifetime. At each time step, the lifetime of the storage and consumption unit is increased by one hour in case of energy deficits in the grid. The same happens for the storage and production unit in case of energy surpluses. After reaching the end of the lifetime, each component is replaced using the same parameters. This is documented in the ChemPlants.txt-file in the folder of the input data as shown in Figure 9-3.

```
################################################
CHEMName                EnegieparkMainz
CHEMID                  1
CHEMActive              1
CHEMStart               01.01.2020
[StorageUnit]
CHEMS_Type              1
CHEMS_Loss              0
CHEMS_nuS               0.7
```

Figure 9-3: Example of a renewed facility for the of the hydrogen and methane storage plant model

9.2 Pre-processing

The input data for the production, the storage and the consumption unit are taken from the literature. The sources of the example set up shown in chapter 9.3 are listed in Appendix Table A 4. The pixel of the plant can be determined by overlaying the GIS-Layer with the mask of the model region. The pixel does not necessarily have to represent the geographical location in the grid. However, no further electrical, chemical or thermal energy storage plants can be placed on the same pixel.

9.3 Input data and Format

The setup file for the hydrogen and methane storage plants is split into the following four sections:

- [General]:

Table 9-1: Description of the input-file for the CHEM-Model, Section General

Input Parameters	Description	Unit	Data format
CHEMName	**Name of the hydrogen and methane storage plant**	**[-]**	**character**
CHEMID	**ID-number of the hydrogen and methane storage plant**	**[-]**	**integer**
CHEMActive	**Status of the HMS-plant 0 – off, 1 – on**	**[-]**	**integer**
CHEMStartYear, CHEMStartMonth, CHEMStartDay	**Start time of the HMS-plant**	**[-]**	**integer**
CHEMProxel	**Pixel**	**[-]**	**integer**

- [ProductionUnit]:

Table 9-2: Description of the input-file for the CHEM-Model, Section ProductionUnit

Input Parameters	Description	Unit	Data format
CHEMP_Type	Type of Hydrogen/Methane production: 1 – Electrolyser	[-]	integer
CHEMP_Pmin	Minimum performance of the hydrogen production unit in % of the nominal performance	[-]	real
CHEMP_P	Nominal performance of the hydrogen production unit	[MW]	real
CHEMP_Prodmin	Production rate of hydrogen at minimum performance	[Nm^3/h]	real
CHEMP_Prod	Production rate of hydrogen at nominal performance	[Nm^3/h]	real
CHEMP_Pres	Pressure of the production flow rate	[bar]	real
CHEMP_LT	Lifetime of the hydrogen production unit	[h]	integer
CHEMP_nuT	Efficiency of the rectifier	[-]	real

- [StorageUnit]:

Table 9-3: Description of the input-file for the CHEM-Model, Section StorageUnit

Input Parameters	Description	Unit	Data format
CHEMS_Type	Type of Storage 1 – Storage in pressure tanks/LOHC/liquid form, 2 – Thermochemical conversion to methane and Storage in pressure tank, 3 –Biological conversion to methane and Storage in pressure tank	[-]	integer
CHEMS_H2FI	Grid Feed in of hydrogen gas 0 – no, 1 – yes	[-]	integer
CHEMS_CH4FI	Grid Feed in of methane gas 0 – no, 1 – yes	[-]	integer
CHEMS_Cap	Capacity of the storage unit	[kg]	real
CHEMS_Loss	Hourly losses of the storage unit	[-]	real
CHEMS_Pres	Pressure of the storage unit	[bar]	real
CHEMS_LT	Lifetime of the storage unit	[h]	integer
CHEMS_nuS	Efficiency of the dis-/charging process, in case of methanation including the efficiencies of the Sabatier-process and the CO_2-generation	[-]	real

- [ConsumptionUnit]:

Table 9-4: Description of the input-file for the CHEM-Model, Section ConsumptionUnit

Input Parameters	Description	Unit	Data format
CHEMC_Type	Type of H2/CH4-Consumption: 1 – Fuel cell or gas-fired plant	[-]	integer
CHEMC_P	Nominal performance of the consumption unit	[MW]	real
CHEMC_nuE	Electrical Efficiency of the consumption unit	[-]	real
CHEMC_WH	Utilization of waste heat 0 – no, 1 – yes	[-]	integer
CHEMC_nuWH	Heat production of the consumption unit related to nominal performance	[-]	real
CHEMC_LT	Lifetime of the consumption unit	[h]	integer

Example setup for a Hydrogen Storage Plant with pressure tanks and complete Grid Feed-In:

```
[General]
ObjectType              CHEM
CHEMName                EnegieparkMainz
CHEMID                  1
CHEMActive              1
CHEMStartYear           2000
CHEMStartMonth          1
CHEMStartDay            1
CHEMProxel              100          200
[end]

[ProductionUnit]
CHEMP_Type              1
CHEMP_Pmin              0
CHEMP_P                 1.25
CHEMP_Prodmin           0
CHEMP_Prod              225
CHEMP_Pres              35
CHEMP_LT                80000
CHEMP_nutT              0.9
[end]

[StorageUnit]
CHEMS_Type              1
CHEMS_H2FI              1
CHEMS_CH4FI             0
CHEMS_Cap               780
CHEMS_Loss              0
CHEMS_Pres              80
CHEMS_LT                175200
CHEMS_nuS               0.7
[end]

[ConsumptionUnit]
CHEMC_Type              0
```

```
CHEMC_P                 0
CHEMC_nuE               0
CHEMC_WH                0
CHEMC_nuWH              0
CHEMC_LT                0
[end]
```

Figure 9-4: Example of the input file for the hydrogen and methane storage plant model

9.4 Output

The output includes the consumed energy of the charging and the obtained energy of the discharging processes, the free storage capacities and the amount of saved energy of the storage facilities, the amount of consumed CO_2 in case of methanation and the amount of gas feed-in into the grid. For cogeneration plants and high-temperature fuel cells, the waste heat of the combustion processes or the transformation is also calculated.

10 Implementation within the Energy Model

The storage model is completely integrated within the energy management component, since the charging and discharging processes are determined from the hourly energy deltas. The working flow within the PROMET model and its components for the calculation of the energy paths is shown in Figure 10-1.

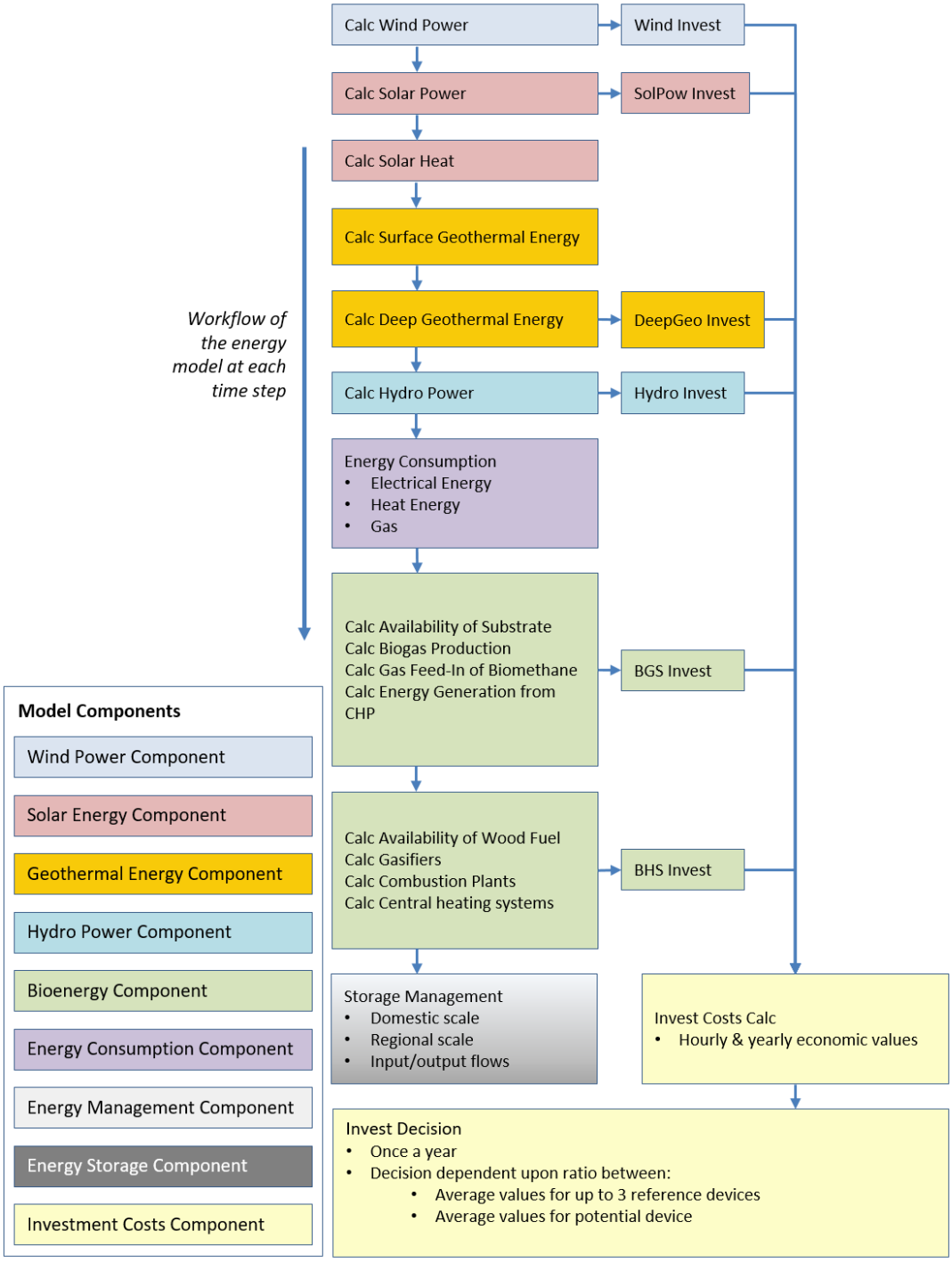

Figure 10-1: Workflow of the Energy model with the regarding components

References

AGRAWAL, P., NOURAI, A., MARKEL, L., FIORAVANTI, R., GORDON, P., TONG, N. AND HUFF, G. 2011: Characterization and assessment of novel bulk storage technologies. A study for the DOE Energy Storage Systems Program. SAND2011-3700. Albuquerque, Livermore: Sandia National Laboratories.

C.A.R.M.E.N. E.V. 2017: (Eds.) Marktübersicht Batteriespeicher. C.A.R.M.E.N. e.V. Centrales Agrar-Rohstoff Marketing- und Energie-Netzwerk,Straubing.

DIN 4708-2:1994-04 (Eds.) Zentrale Wassererwärmungsanlagen; Regeln zur Ermittlung des Wärmebedarfs zur Erwärmung von Trinkwasser in Wohngebäuden (4708-2:1994-04).

DIN EN 12831-1:2017-09 (Eds.) Energetische Bewertung von Gebäuden - Verfahren zur Berechnung der Norm-Heizlast. (EN 12831-1:2017-09).

FLOß, A. AND DIETRICH, C. H. B. INSTITUT FÜR GEBÄUDE- UND ENERGIESYSTEME (Eds.) Optimierte Integration von Pufferspeichern.

FRENZEL, I., JARASS, J., TROMMER, S. AND LENZ, B. 2015: Erstnutzer von Elektrofahrzeugen in Deutschland. Nutzerprofile, Anschaffung, Fahrzeugnutzung. Berlin: Deutsches Zentrum für Luft- und Raumfahrt e. V. (DLR).

GIESECKE, J. AND MOSONYI, E. 1998: Wasserkraftwerke – Planung, Bau und Betrieb. . Springer Verlag Berlin Heidelberg.

GRAVITY POWER 2017: Gravity Power. Grid Scale Energy Storage. Available at: http://www.gravitypower.net/ (Access date: 12.12.2017).

HACKER, F., BLANCK, R., HÜLSMANN, F., KASTEN, P., LORECK, C., LUDIG, S., MOTTSCHALL, M. AND ZIMMER, W. 2014: eMobil 2050. Szenarien zum möglichen Beitrag des elektrischen Verkehrs zum langfristigen Klimaschutz. Berlin: Öko-Institut e.V. .

HARTMANN, H., REISINGER, K., TUROWSKI, P. AND ROßMANN, P. 2013: Handbuch Bioenergie-Kleinanlagen Gülzow: Fachagentur Nachwachsende Rohstoffe (FNR).

HAUER, A., HIEBLER, S. AND REUß, M. 2013: Wärmespeicher. Fraunhofer IRB Verlag, Bonn.

HEINDL ENERGY GMBH 2017: Gravity Storage. A new StoreAge. Available at: www.heindl-energy.com (Access date: 23.01.2017).

HIRSCHER, M. 2010: Handbook of hydrogen storage: New Materials for future Energy Storage. Wiley-VCH Verlag GmbH & Co. KGaA, Weinheim.

JÜLICH, V., THOMSEN, J., HARTMANN, N., JUNNE, T., UNTERREINER, L., ARNOLD, M., REITH, S., ELTROP, L., WASSERMANN, S. AND NIEDERBERGER, M. 2016: Betreibermodelle für Stromspeicher - Ökonomisch-ökologische Analyse und Vergleich von Speichern in

autonomen, dezentralen Netzen und für regionale und üebrregionale Versorgungsaufgaben. Förderungsbericht BWPLUS.

LI, C.-H., ZHU, X.-J., CAO, G.-Y., SUI, S. AND HU, M.-R. 2009: Dynamic modeling and sizing optimization of stand-alone photovoltaic power systems using hybrid energy storage technology. *Renewable energy*, 34(3), 815-826.

MAINZER STADTWERKE AG 2017: Energiepark Mainz - Technische Daten. Available at: http://www.energiepark-mainz.de/wissen/technische-daten/ (Access date: 10.04.2017).

MANGOLD, D., BENNER, M. AND SCHMIDT, T. 2001: (Eds.) Langzeit-Wärmespeicher und solare Nahwärme. Fachinformationszentrum Karlsruhe, Gesellschaft für wissenschaftlich-technische Information mbH,Eggenstein-Leopoldshafen.

OCHSNER, K. 2009: Wärmepumpen in der Heizungstechnik: Praxishandbuch für Installateure und Planer. Müller.

OPIYO, N. 2016: Energy storage systems for PV-based communal grids. *Journal of Energy Storage*, 7, 1-12.

PETER, S. 2013: Modellierung einer vollständig auf erneuerbaren Energien basierenden Stromerzeugung im Jahr 2050 in autarken, dezentralen Strukturen. Dessau-Roßlau: Umweltbundesamtes (UBA).

SCHABBACH, T. AND LEIBBRANDT, P. 2014: Solarthermie: Wie Sonne zu Wärme wird. Springer-Verlag.

SCHOOP, E. 2013: Stationäre Batterieanlagen. Auslegung, Installation und Wartung. HUSS-Medien Berlin.

SIEMENS AG 2017: (Eds.) SILYZER 200 - Mit Hochdruck effizient im Megawattbereich. Broschüre.Nürnberg.

SOLITES 2014: Saisonalspeicher.de Das Wissensportal für die saisonale Wärmespeicherung. Available at: www.saisonalspeicher.de (Access date: 17.5.2017).

STERNER, M. AND STADLER, I. 2014: Energiespeicher - Bedarf, Technologien, Integration. Springer-Verlag Berlin Heidelberg.

STROBL, T. AND ZUNIC, F. 2006: Wasserbau. Aktuelle Grundlagen - Neue Entwicklungen. Springer, Berlin Heidelberg.

WENIGER, J., TJADEN, T. AND QUASCHNING, V. 2014: Sizing of residential PV battery systems. *Energy Procedia*, 46, 78-87.

WILLEMS, W., KASPER, G. AND KLOTZ, P. 2007: DANUBIA Software Documentation. GLOWA-Danube Papers. Technical Release No. 12. Software-Release-No.: 1.2.6 Documentation Version: 2.2.

Appendix

Table A 1: Heat loss rates for selected Storage volumes according to PETER (2013)

Storage volume [l]	Heat loss rate [W/K]
300	2.00
1.450	4.20
2.900	6.77
4.00	9.33
10.000	9.50
100.000	50.00
1.000.000	250.00

Table A 2: Storage capacities for the four different STES-types (Mangold, et al. 2001)

Storage Type	Storage Capacity per m^3 p_{ST}
Hot Water Thermal Energy Storage	70
Gravel-Water Thermal Energy Storage	40
Borehole thermal energy storage	22.5
Aquifer thermal energy storage	35

Table A 3: Storage capacities for the four different Seasonal Thermal Energy Storage types (Mangold, et al. 2001)

Storage Type	Storage volume for 1 m^3 water equivalent sv
Hot Water Thermal Energy Storage	1
Gravel-Water Thermal Energy Storage	1.65
Borehole thermal energy storage	4
Aquifer thermal energy storage	2.5

Table A 4: Literature sources of the example input setup of the Hydrogen Storage Plant

Input Parameters	Source
CHEMP_Pmin, CHEMP_P, CHEMP_Prodmin, CHEMP_Prod, CHEMP_Press, CHEMP_LT	SIEMENS AG (2017)
CHEMP_nuT	STERNER AND STADLER (2014)
CHEMS_Cap, CHEMS_Press	MAINZER STADTWERKE AG (
CHEMS_Loss	HIRSCHER (2010)
CHEMS_LT , CHEMS_nuS	LI, et al. (2009)